

M. Tech (cs)

Characterisation of architectural distortion in Mammograms

A dissertation submitted in partial fulfillment of the requirements
for the M. Tech(cs) degree of the Indian Statistical Institute

By

Vaibhav Tyagi

Under the supervision of

Bhabatosh Chanda

Indian Statistical Institute
203, B.T. Road,
Kolkata - 108



**Indian Statistical Institute,
Kolkata, 700 108**

CERTIFICATE

This is to certify that the thesis entitled "*Characterisation of Architectural Distortion in Mammograms*" is submitted in partial fulfillment of the requirement for the award of the degree of the Masters in Technology in *Computer Science* at Indian Statistical Institute, Kolkata.

It is a faithful record of bona fide research work carried out by Mr. Vaibhav Tyagi (mtc0521) under my supervision and guidance. It is further certified that no part of thesis has been submitted to any other University or Institute for the award of any Degree or Diploma.

(Professor Bhabatosh Chanda)
Supervisor

Countersigned
External Examiner

Date: of July, 2007.

Acknowledgements

With great pleasure and sense of obligation I express my heartfelt gratitude to my guide and supervisor **Prof. Dipti Prasad Mukherjee** of Electronics and Communication Science Unit, Indian Statistical Institute, Kolkata. I am highly indebted to him for his invaluable guidance and ever ready support. His persisting encouragement, perpetual motivation, everlasting patience and excellent expertise in discussions, during progress of Project Work, have benefited to an extent, which is beyond expression.

I would also like to sincerely thank **Prof. Bhabatosh Chanda** of same unit, for his invaluable time, assistance, guidance and encouragement while supervising me in the absence of my guide, and helping me to finalise this project to its conclusion.

The chain of my gratitude would be definitely incomplete without expressing my gratitude to all my batch mates, for their support and encouragement throughout the entire M.Tech course. Lastly I sincerely thank all my friends and well wishers who helped me directly or indirectly towards the completion of this work.

Vaibhav Tyagi,

mtc0521,

Indian Statistical Institute,

Kolkata 700 108.

Abstract

Architectural Distortion is a very important finding in interpreting breast cancers as well as microcalcification and mass on digital mammograms. During screening mammography, architectural distortion is generally missed because of its subtlety; however architectural distortion has high potential for malignancy. Computer-aided diagnosis (CAD) techniques can improve the performance of radiologists in detecting masses and calcifications, however, most CAD systems have not been designed to detect architectural distortion.

The objective of this work is to develop an automated image processing algorithm to detect architectural distortion in digital mammograms based on irregular concentration of mammary gland. Digital image of a breast in mammogram is modeled as a topographic image intensity surface whose contour map is used to find the linear structures of the mammary glands. The irregular concentration of these linear structures is indicative of architectural distortion being present in a mammogram.

The proposed approach was tested on various mammograms from mini-MIAS database containing both normal and architectural distortion cases and the initial results are promising. The methodology needs to be rigorously tested on a larger database, so as to be of greater practical use.

Contents

Chapter I Introduction	vii
1.1 Early Detection and Mammograms	viii
1.1.1 Mass lesion:.....	x
1.1.2 Micro-calcification:.....	x
1.1.3 Architectural Distortion:.....	x
1.2 Challenges in Mammography	xi
1.3 Contribution and Organization of the thesis	xvii
1.4 Summary	xvii
Chapter II Methodology	xviii
2.1 Binarization Process-finding linear structures	xx
2.1.1 Implementation:.....	xx
2.2: Concentration Index (CI):	xxi
2.2.1: Quantitative Measurement of Concentration	xxii
2.2.2: CI filter on the digital Image	xxiii
2.2.3: Properties of the CI:.....	xxiv
2.2.4: Implementation:.....	xxiv
2.3: Summary	xxvii
Chapter III Results and Discussions	xxviii
3.1 Summary	xxxiiii
Chapter IV Conclusion and Future Scope	xxxiv
Appendix A	xxxv
References	xxxvii

List of Figures

Figure 1 A mammogram showing a normal breast, from the Mini-MIAS database (mdb243).....	xiii
Figure 2 Architectural distortion present in a mammogram from the mini-MIAS database (mdb115).....	xiv
Figure 3 A detail of mammogram mdb115 showing the architectural distortion site marked by the box in Figure 2.....	xv
Figure 4 Simplified illustration of (a) normal image, (b) architectural distortion's image with concentration of mammary gland (center), and (c) areas for calculating concentration index of mammary gland.....	xix
Figure 5 Illustrative example of line pattern textures.....	xxi
Figure 6 Illustration of Concentration Index.....	xxiii
Figure 7 Line elements in a digitized line pattern.....	xxiv
Figure 8 A synthetic image having two lines along the diagonal.....	xxvi
Figure 9 CI for Figure 8.....	xxvi
Figure 10 Line elements for ROI selected from mdb115 of mini- MIAS database.....	xxix

Figure 11 CI for ROI selected from the mdb115 of mini-MIAS
database.....xxx

Figure 12 Line Pattern for ROI selected from mdb129 of mini-MIAS
database.....xxxi

Figure 13 CI for ROI selected from the mdb129 of mini-MIAS
database.....xxxii

Chapter - I
Introduction

Introduction

Breast Cancer is the second leading cause of cancer deaths in women today (after lung cancer) and is the most common cancer among women, excluding nonmelanoma skin cancers. According to the World Health Organization, more than 1.2 million people will be diagnosed with breast cancer each year worldwide. The American Cancer Society estimates that 178,480 new cases of invasive breast cancer will be diagnosed in 2007. About 40,910 breast cancer deaths are expected in 2007. According to the American Cancer Society, the chance that breast cancer will be responsible for a woman's death is about 1 in 33 [1].

According to National Cancer Institute of Canada, the lifetime probability of the development of breast cancer in women in Canada is 1 in 8.8, with a lifetime probability of 1 in 27.4 of dying due to the disease [2]. In the western world, this percentage is 27% and about 1 in 10 to 12 women will have to face breast cancer. In most European countries the aged standardised mortality rates for breast cancer range from 15 to 30 for every 100,000 women making breast cancer the most important cause of cancer-related mortality for women [3].

1.1 Early Detection and Mammograms

Screening Mammography is the best available tool for detecting early breast cancer, screening programs have been shown to reduce mortality rates by 30-70% [4],[5, Ch 19]. Mammography is an X-ray technique developed specifically for the breast. It is based on the differential

absorption of X-rays between the various tissue components of the breast such as fat, connective tissue, tumor tissue and calcifications.

One of the most recent advances in x-ray mammography is digital mammography. Digital (computerized) mammography is similar to standard mammography in that x-rays are used to produce detailed images of the breast. Digital mammography uses essentially the same mammography system as conventional mammography, but the system is equipped with a digital receptor and a computer instead of a film cassette. With digital mammography, the magnification, orientation, brightness, and contrast of the image may be altered after the exam is completed to help the radiologist more clearly see certain areas [1].

Mammography is used both as a clinical tool to examine symptomatic patients and for screening. Screening mammographic examinations are performed on asymptomatic woman to detect clinically unsuspected breast cancer early. Two views of each breast are recorded; the *craniocaudal* (CC) view, which is top to bottom view, and *mediolateral oblique* (MLO) view, which is side view taken at an angle. Requirements for mammography are *high* contrast, *high* spatial resolution, and *minimal* radiation exposure. High contrast is needed because differences in density between normal and pathologic structures of the breast are small. The detection of micro-calcifications requires both high contrast as well as a high spatial resolution. Minimal radiation exposure is essential as in screening programmes women frequently undergo mammography, often annually or bi-annually.

Radiologists visually search mammogram for specific abnormalities. Some of the important signs of breast cancer that

radiologists look for are clusters of micro-calcifications, masses and architectural distortions.

1.1.1 Mass lesion: Most breast tumors, benign as well as malignant ones, present as a focal mass lesion. The most important sign of malignancy is the presence of spiculation. This is a stellate pattern of lines directed towards the centre of a lesion. The border of a mass may also give information about the potential malignancy of a lesion. Benign masses are often characterised by sharp, circumscribed borders. Malignant masses on the other hand frequently have ill-defined or spiculated borders.

1.1.2 Micro-calcification: Another sign of malignancy is the presence of micro-calcifications. These are tiny deposits of calcium, which appear as small bright spots on the mammograms. They are characterised by their type and distribution properties.

1.1.3 Architectural Distortion: It is defined in BI-RADS [6] as follows: *“The Normal Architecture (of the breast) is distorted with no definite mass visible. This includes spiculations radiating from a point and focal retraction or distortion at the edge of the parenchyma”*

Architectural distortion could be categorized as malignant or benign; the former includes cancer while the latter includes scar and soft-tissue damage due to trauma. According to van Dijck et al. [7], “in nearly half of the screen-detected cancers, minimal signs appeared to be present on the previous screening mammogram 2 years before the diagnosis.” Burrell et al. [8], in a study of screening interval breast cancers, have

showed that architectural distortion is the most commonly missed abnormality in false-negative cases. Sickles [9] has reported that indirect signs of malignancy (such as architectural distortion, bilateral asymmetry, single dilated duct, and developing densities) account for almost 20% of the detected cancers. Broeders et al. [10] have suggested that improvement in the detection of architectural distortion could lead to an effective improvement in the prognosis of breast cancer patients.

1.2 Challenges in Mammography

Early detection via mammography increase breast cancer treatment options and the survival rate. However, mammography is not perfect. Detection of suspicious abnormalities is a repetitive and fatiguing task. For every thousand cases analysed by a radiologist, only 3 to 4 are cancerous and thus an abnormality may be overlooked. As, a result, radiologists fail to detect 10-30% cancers [11-13]. Approximately two-thirds of these false negative results are due to missed lesions that are evident retrospectively [14]. Due to considerable amount of overlap in the appearance in the malignant and benign abnormalities, mammography has a positive predictive (PPV) value of less than 35% [15], where PPV is defined as the percentage of lesions subjected to biopsy that were found to be cancer. Thus a high number of biopsies are performed on benign lesions. Avoiding benign biopsies would spare women anxiety, discomfort, and expense.

CAD systems have been developed to aid radiologists in detecting mammographic lesions that may indicate the presence of breast cancer. These systems act only as second reader and final decision is made by the radiologist. It is important to realize that mammographic image analysis

is an extremely challenging task for a number of reasons. First, since the efficiency of CAD systems can have serious implications, there is need for near perfection. Second, the large variability in the appearance of the abnormalities makes this a very difficult image analysis task. Finally, abnormalities are often occluded or hidden in dense breast tissues, which make detection difficult. However, current CAD systems are devised to detect masses and micro-calcifications, and hence they work poorly at the task of detecting other less prevalent but clinically significant lesion types, particularly *architectural distortions*. Figures 1 and 2 depict two mammograms with and without architectural distortions from mini-MIAS database. Figure 3 shows the region of interest of the mammogram image of Figure 2 that includes an architecturally distorted region identified by radiologist [16].

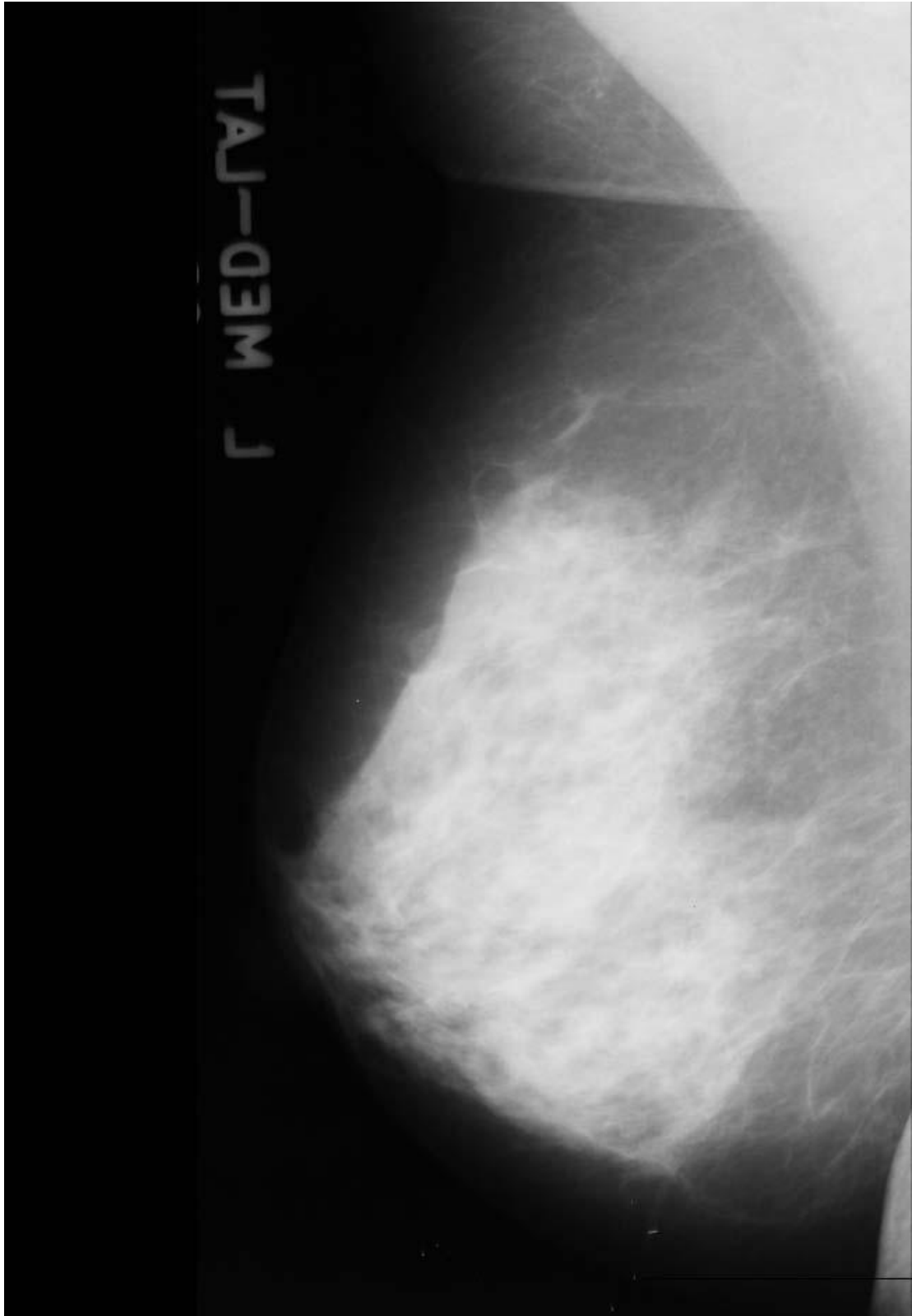


Figure 1: A mammogram showing a normal breast, from the Mini-MIAS database (mdb243).

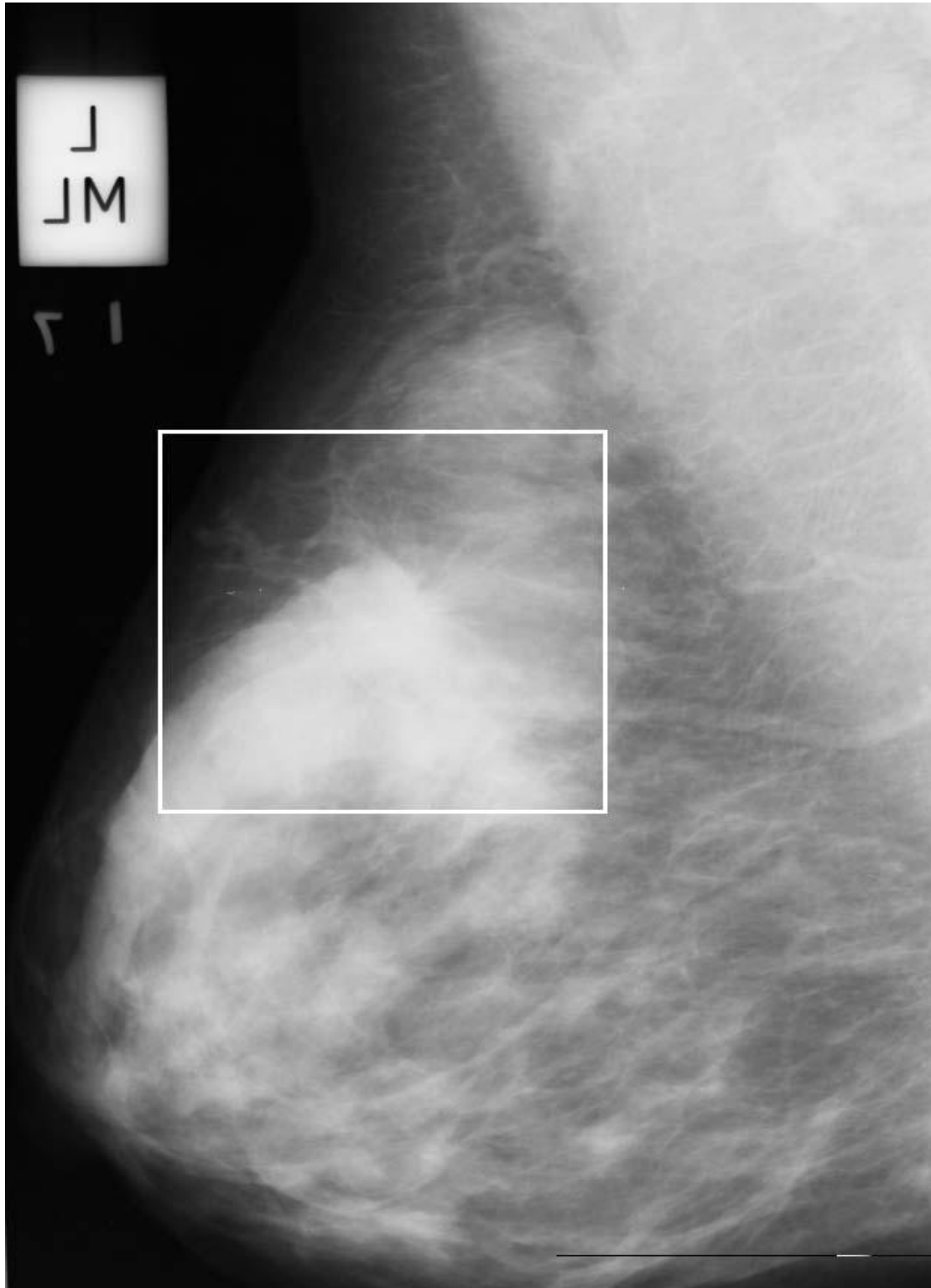


Figure 2: Architectural distortion present in a mammogram from the mini-MIAS database (mdb115). The square box overlaid on the figure represents the region of interest (ROI) including the site of architectural distortion (enlarged in Figure 3).

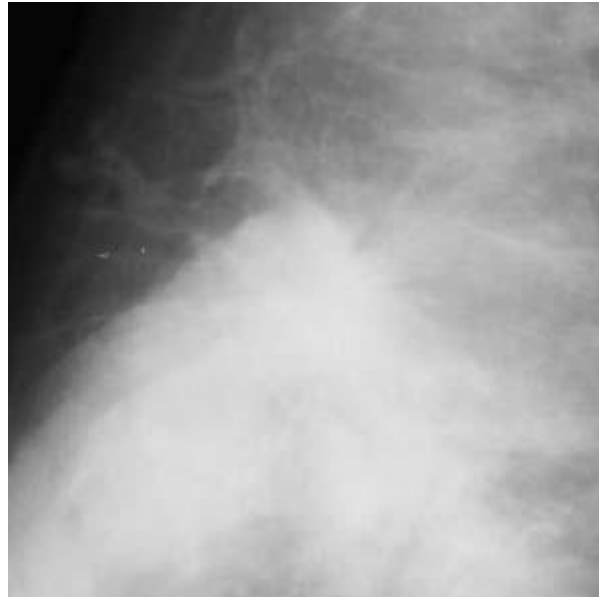


Figure 3: A detail of mammogram mdb115 showing the architectural distortion site marked by the box in Figure2.

The breast contains several piecewise linear structures, such as ligaments, ducts, and blood vessels, that cause directionally oriented texture in mammogram. The presence of architectural distortion is expected to change the normal oriented texture of the breast. To address the problem of detecting architectural distortion in a mammogram several methods exist in literature.

Ayres and Rangayyan [17] have used phase portraits to characterize architectural distortion in mammograms. They have used Gabor filters to detect linear patterns and the orientation of local texture in mammograms. The results of Gabor filtering is then analysed using phase portraits. A linear discriminant classifier is used to classify whether ROIs contains architectural distortion or other parenchymal patterns.

Eltonsy et al. [18] have utilized morphological effects on breast parenchyma due to cancer infiltration, to characterize architectural

distortion in mammograms. The main morphological features used by them are area, solidity, extent and eccentricity.

Guo et al. [19] have applied support vector machine to detect architectural distortion in mammograms. They have used Hausdroff dimension to characterize the texture feature of mammograms.

Tourassi et al. [20] have explored the application of fractal analysis to the investigation of architectural distortion in screening mammograms.

Whitman et al. [21] have developed a new class of linear filters, named Radial Spiculation Filters (RSF) to detect architectural distortion in mammograms. These RSF are applied on an enhanced image obtained by filtering mammogram in the Radon domain.

Rashed et al [22] have used wavelet multilevel decomposition to transform a mammogram into a feature vector. This vector is then used to train a multi-layer perceptron to detect architectural distortion in a mammogram.

Zaiane et al. [23] have used Association rule mining classification technique to classify a mammogram into three classes- normal, benign, and malign.

Matsubara et al. [24-26] have used mathematical morphology to detect architectural distortion around the skin line and a concentration index to detect architectural distortion within the mammary gland.

1.3 Contribution and Organization of the thesis

The approach taken in this project is a modification of Matsubara et al [24-26] methodology for detecting architectural distortion within the mammary gland. Efforts have been made to utilize contour information from a mammogram. Contour information can give better continuous linear structure information which is not possible from existing Matsubara technique which uses different shape filters.

The thesis is organized as follows. Chapter 2 explains the methodology used in this project. Chapter 3 deals with the results and discussion thereof. Chapter 4 contains the conclusion and future scope of present proposal.

1.4 Summary

Breast Cancer is a major cause of cancer deaths in women today. Screening Mammography is an X-ray technique developed specifically for the breast, and is the best available tool for detecting early breast cancer. Out of various indications of breast cancer, architectural distortion is the most commonly missed abnormality in false-negative cases. Present day CAD systems work poorly at the task of detecting less prevalent but clinically significant lesion types, particularly architectural distortion. Several approaches to detect architectural distortion in mammograms exist. The next chapter explains the methodology used in this thesis to detect architectural distortions.

Chapter II
Methodology

Methodology

The images of mammary glands in mammograms are approximated by linear structures. The distributions of mammary glands can be approximated by the distribution of these linear structures. The mammary glands within normal breast are towards the nipple; on the other hand, those within abnormal breast are usually towards the suspect area. A schematic is shown in Figure 4. The suspect area is determined by concentration index (CI) calculated by lengths, directions, and distances of the linear structure [24-26]. CI is a kind of nonlinear filter which calculates at each pixel the degree of concentration of line patterns to that pixel. The concentration index of the distorted area has a high value because the linear structures of the mammary gland are towards the suspect area.

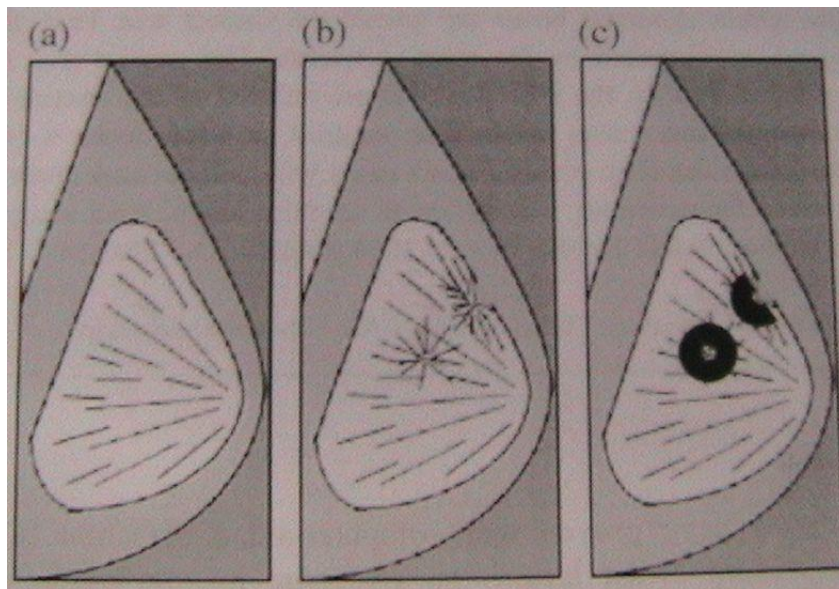


Figure 4: Simplified illustration of (a) normal image, (b) image of architectural distortion with concentration of mammary gland (center), and (c) areas for calculating concentration index of mammary gland [25].

2.1 Binarization Process-finding linear structures

To find the linear structures in a mammogram, intensity image of a breast is modeled as topographic surface. The contour map of mammogram (see section 2.1.1), obtained by considering isolines at various intensities, contain information about the intensity distribution in mammograms, which are gray-scale images. This intensity distribution can be utilized to identify the suspicious region. The underlying assumption is that, the distorted tissues tend to be light areas (white/bright regions on films); on the other hand, the surrounding regions around the architectural distortions are dark because these areas contain considerable amount of fat tissue. As a result the regions of architectural distortions are expected to be enclosed within closed contours, with broken, incomplete or no contours of significant length within.

2.1.1 Implementation: Let $I(x, y)$ be the gray value of mammogram of size $row \times column$, i.e. $0 \leq x \leq row$ and $0 \leq y \leq column$. For the mammograms considered in this project $I(x, y) \in \{0, 1, \dots, 255\}$

and let $Max = Maximum\{I(x, y)\} - 1$

$$Min = Minimum\{I(x, y)\} + 1$$

Let $C(x, y)$ be a matrix of same size as $I(x, y)$ and initialized to zero. $C(x, y)$ is the contour map of the mammogram.

Divide the interval $Max - Min$ in ' t ' equal parts ($t = 10$ is a good choice, determined experimentally) and form images $I_j(x, y)$ for $j = 1, 2, \dots, t$ where

$$I_j(x, y) = \begin{cases} 1, & \text{if } I(x, y) < \text{Min} + (j-1) * (\text{Max} - \text{Min}) / t \\ 0, & \text{otherwise} \end{cases} \quad (2.1)$$

Now find the boundary of the binary image $I_j(x, y)$ for each j . Add the boundary of $I_j(x, y)$ to $C(x, y)$ to obtain total contour map of the mammogram at j^{th} step. Also perform thinning [27] of $C(x, y)$ after each addition of boundary of $I_j(x, y)$ to keep contours single pixel thick.

For each contour in $C(x, y)$, calculate its length and eliminate those contours whose lengths are less than a chosen threshold (10 pixels in current work). The resulting contour image so obtained is taken for the calculation of concentration index.

2.2: Concentration Index (CI): CI is a kind of nonlinear filter which is applicable to local feature extraction of complicated linear texture pattern [28]. This filter calculates at each pixel the degree of concentration of line pattern to that pixel. Let us consider the line pattern as shown in Figure 5.

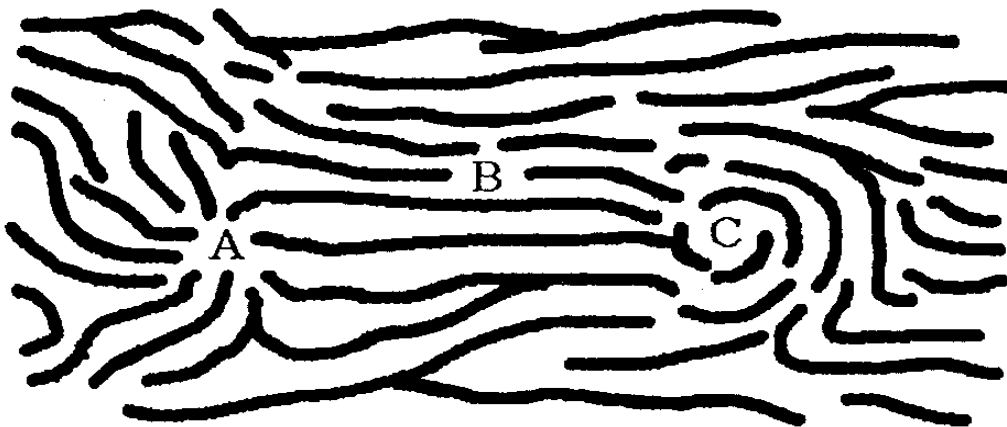


Figure 5: Illustrative example of line pattern textures [28].

Local patterns in Figure 5 have different features at different places. In the neighborhood of point ‘A’, for example, curved lines look like concentration at the point ‘A’. In the neighborhood of ‘B’, on the other contrary, none of such concentration is observed, and all the lines run in parallel to each other.

2.2.1: Quantitative Measurement of Concentration: Suppose that a binary line pattern is given in the continuous plane \mathbb{R}^2 . Let us consider an arbitrary pattern P , its neighborhood R in the plane, and a arbitrary point Q on a line pattern in R . Then the contribution by the small line element at Q towards the concentration of the pattern on the point P is given by

$$dx|\cos\alpha|/r \quad (2.2)$$

where dx is the length of a line element at the point Q ,

α is the angle between the line element and line segment \overline{PQ} , and

r is the distance between P and Q .

The value given by *equation 2.2* is regarded as the contribution to concentration index, by the small line element at Q towards the point P . Basing upon this measure, Concentration Index CI at a point P is defined as follows (Figure 6):

$$CI(P) = \frac{\sum_R (dx|\cos\alpha|/r)}{\sum_R (dx/r)} \quad (2.3)$$

where \sum_R = summation over all points on the line patterns in the neighborhood R . This index means that the magnitude of the component of a line element at Q directed to the point P is weighted by the inverse of the distance from Q to P and is summed over the local area R . The summation is normalized by the sum of the length of the line element

weighted by the inverse of the distance \overline{PQ} so that the effect of the total length of the pattern in the area R is cancelled.

This index is calculated at all points in the image; therefore, such operation of calculating CI is regarded as a kind of local operation or a nonlinear filter for image processing.

2.2.2: CI filter on the digital Image: In this thesis on a digital image, line element is defined as follows. Let us consider a digitized binary line pattern. Every 1-pixel on a line pattern (assuming 8-connectivity for line patterns) is classified by the method in [29] into four types- edge point, connecting point, branch point and crossing point. The line element is defined only at a connecting point. A connecting point always has two adjacent 1-pixels in its 8 neighborhood. Therefore, letting Q_1 and Q_2 be two 1-pixels adjacent to a connecting point Q_0 , assign to Q_0 a line element $l(dx, \theta)$ by the following rule (Figures 6 and 7)

- dx (length of the line element at Q_0)
 - = half of length of the segment $\overline{Q_1Q_2}$
- θ (direction of the line element at Q_0)
 - = direction of line segment $\overline{Q_1Q_2}$.

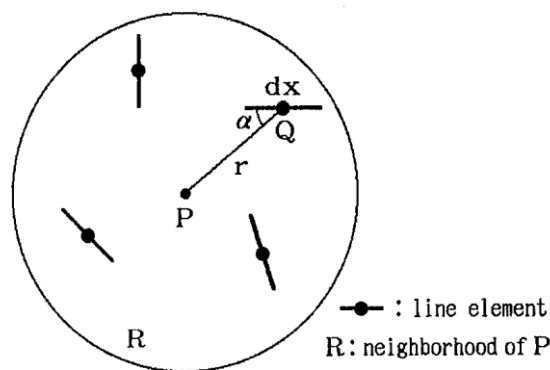


Figure 6 Illustration of Concentration Index [28].

Note that only four types of line elements shown in Figure 7 may exist except configurations symmetric (i.e. 12 more) to them in suitable sense (see Appendix A for all such patterns).

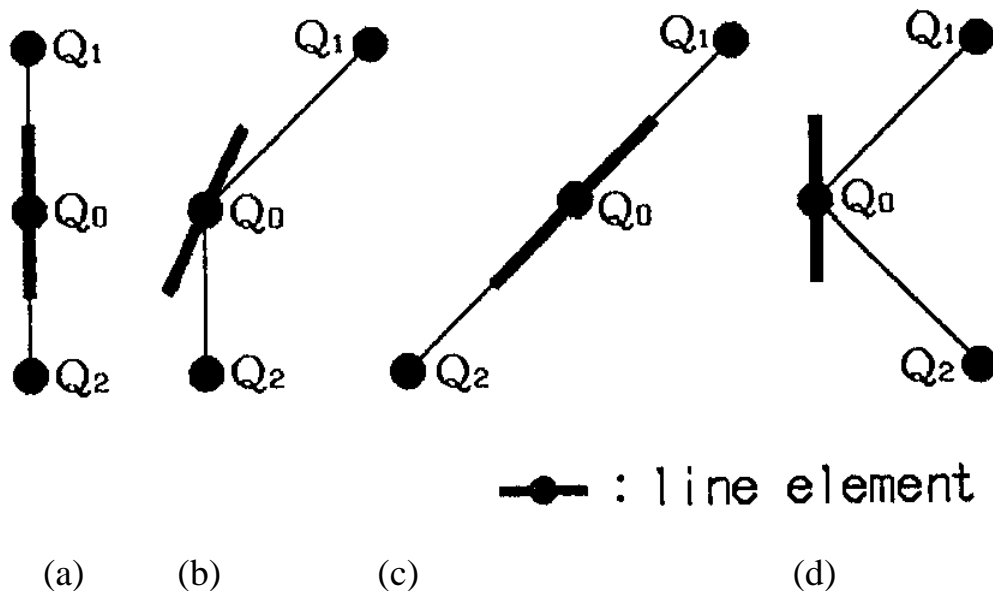


Figure 7 Line elements in a digitized line pattern as defined in this thesis.

2.2.3: Properties of the CI: CI has the following properties

- 1) $0 \leq CI \leq 1$
- 2) If a line pattern in the neighborhood R consists of straight line patterns passing through the point P , then CI at P is 1.
- 3) If a line pattern in the neighborhood R consists of circle with the common center point P , CI at P is equal to 0.

2.2.4: Implementation: Once we have the contour map $C(x, y)$ of a mammogram, from section 2.1, we examine the 8-neighborhood of each 1-pixel (contour pixel) to determine whether it is a connecting pixel or not. Based on this information a label-map $L(x, y)$ is created, where $L(x, y)$ is of size $row \times column$.

$$L(x, y) = 0 \quad \text{if } C(x, y) \text{ is not a connecting pixel}$$

$$= i \quad \text{if } C(x, y) \text{ is a connecting pixel of type } i.$$

where $i \in \{1, 2, \dots, 16\}$. Refer Appendix A for 16 connecting pixel types.

Now at each location P of $L(x, y)$, labels of connecting pixels in the neighborhood R are observed and CI is calculated to form another same sized image $CI(x, y)$ using *equation 2.3*. Note that for a connecting pixel of type i the values of dx and θ are fixed. Thus values of dx and θ need not be calculated each time a connecting pixel of type i is encountered in neighborhood R . For example consider the line element $l(dx, \theta)$ for case (a) in Figure 7.

Here $dx =$ half of length of the segment $\overline{Q_1Q_2}$

$$= 2\text{pixel}/2 = 1 \text{ pixel.}$$

$\theta =$ direction of line segment $\overline{Q_1Q_2}$.

$$= 90^\circ$$

Figure 8 is a synthetic image of size 11×11 with 1-pixel lying on diagonals in the upper half of the figure. Figure 9 shows the CI for Figure 8, with R as entire image.

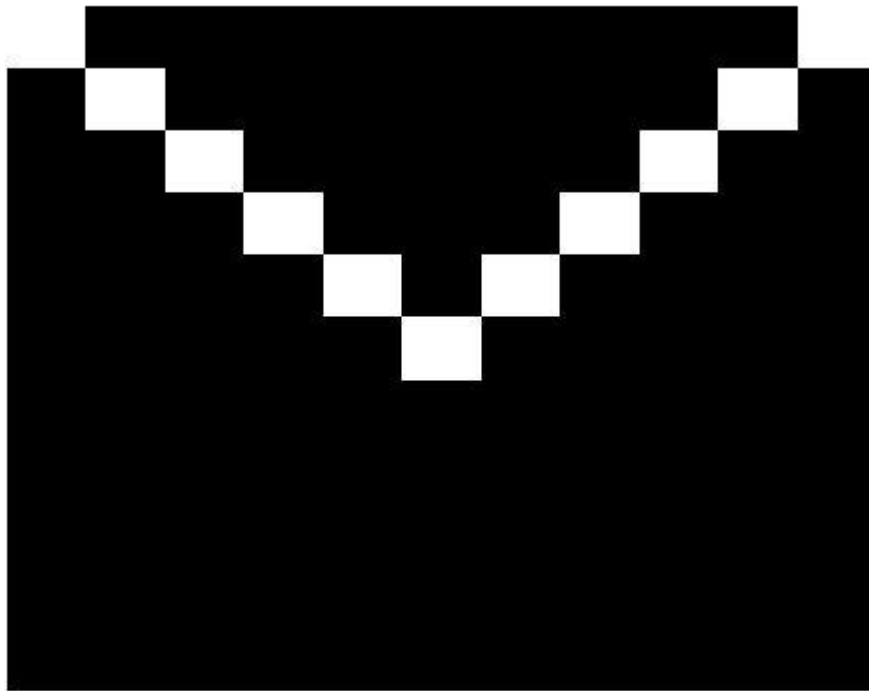


Figure 8 A synthetic image having two lines along the diagonal.

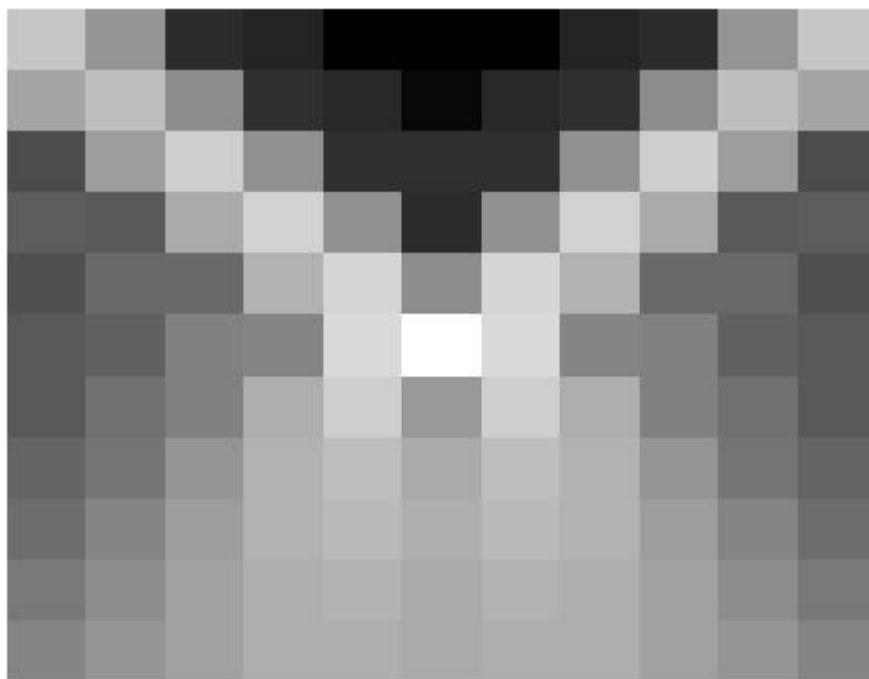


Figure 9 CI for Figure 8.

As can be seen from Figure 9 the intersection point of two diagonals is brightest, since the value of CI at intersection point is 1(maximum) by property 2 (section 2.2.3).

2.3: Summary

Mammary glands within breast are approximated by linear structures. To find the linear structures in a mammogram intensity image of a breast is modeled as topographic surface. The contour map of mammogram is used to find the concentration index due to linear structures within mammograms. The suspect area is determined by concentration index (CI) calculated by lengths, directions, and distances of the linear structure. Results of the proposed scheme are discussed in chapter 3.

Chapter III
Results and Discussions

Results and Discussions

In this chapter the output of the methodology explained in Chapter 2, when applied to a mammogram is presented. Figure 10 shows the linear structures obtained after the binarization step (section 2.1), for the Region of Interest (ROI) selected from mammogram mdb115 of mini-MIAS database (Figure 1). The ROI here corresponds to the entire breast, but any ROI can be selected.

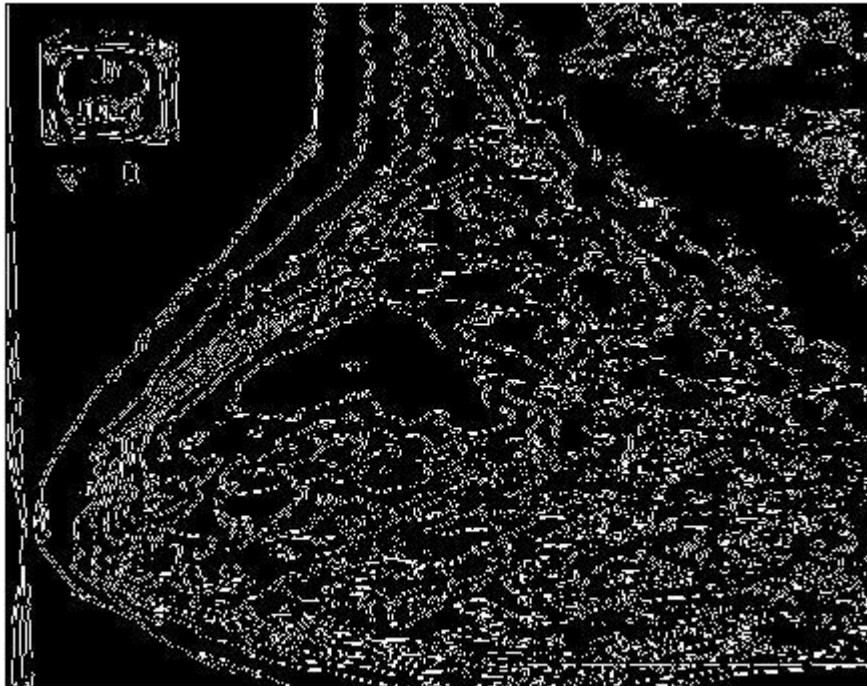


Figure10 Line elements for ROI selected from mdb115 of mini- MIAS database.(with $Max = 244$; $Min = 15$; $t = 10$.)

Figure 11 shows the Concentration Index for the Figure 10. The neighborhood R chosen to calculate CI is window of size 20×20 pixels centered at the pixel at which CI is being calculated. As can be seen the

CI image contain islands of black pixels surrounded by brighter pixels. These black islands are potential sites for architectural distortions. As mentioned earlier, the distorted tissues tend to be light areas (white/bright regions on films); on the other hand, the surrounding regions around the architectural distortions are dark because these areas contain much fat tissue. Due to this reason architectural distortion sites are expected to be enclosed within a contour, and since we have eliminated contours smaller than a specific length (10 pixels in present work), no contours are expected within a region of architectural distortion.

A few of them are definitively false positive like the region of pectoral muscle, enclosed in red quadrilateral, observed at top right side of the image. The actual architectural distortion site (according to the information available in mini-MIAS database) is also enclosed in red quadrilateral and can be seen in the middle of the image.

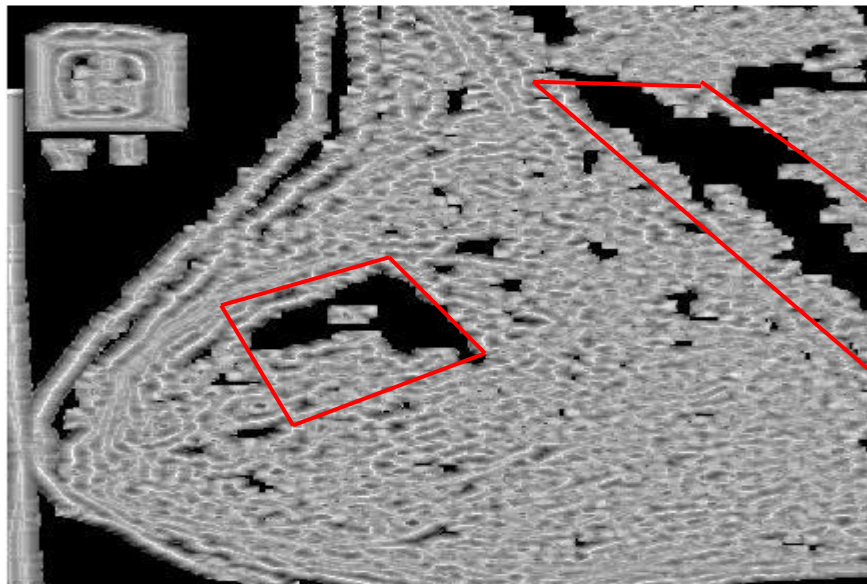


Figure 11 CI for ROI selected from mdb115 of mini- MIAS database (with R as a window of size 20×20).

Figure 12 and Figure 13 shows the result for mammogram mdb129, which is classified as normal in mini-MIAS database, for illustration purpose.

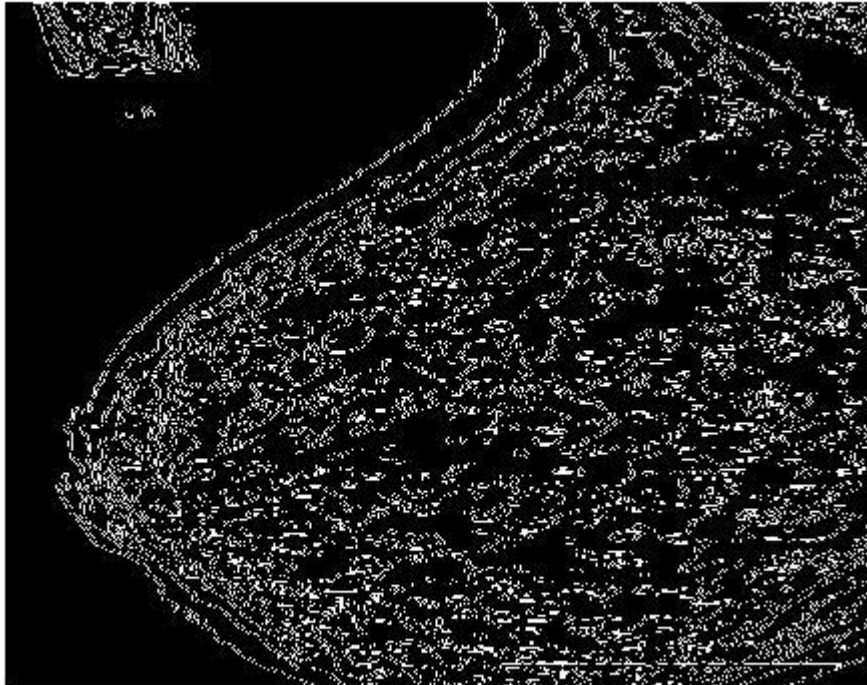


Figure 12 Line Pattern for ROI selected from mdb129 of mini-MIAS database (with $Max = 238$; $Min = 15$; $t = 10$).

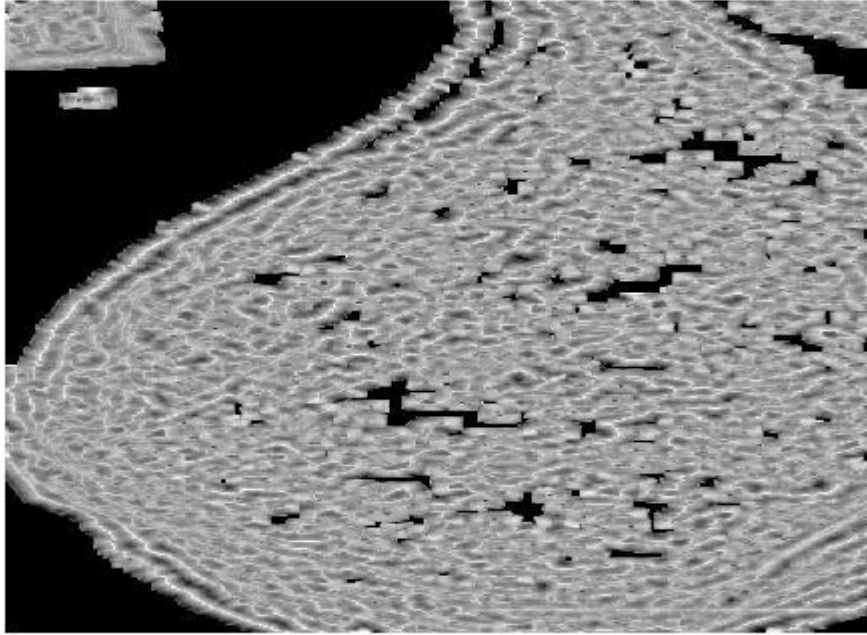


Figure 13 CI for ROI selected from mdb129 of mini- MIAS database (with R as window of size 20×20).

Table 1 shows the result of proposed methodology on 10 different mammograms from mini-MIAS database. According to mini-MIAS database, 5 of these mammograms are of normal breasts and other five have architectural distortion present in them.

Table 1

<i>Mammogram Number</i>	<i>Type as per mini-MIAS database</i>	<i>Max</i>	<i>Min</i>	<i>t</i>	<i>Window size of neighborhood R</i>	<i>No. of False Positive</i>	<i>Whether AD detected</i>
mdb115	ARCH	244	15	10	20×20	1	Yes
mdb129	NORM	238	15	10	20×20	3	-NA-
mdb079	NORM	232	15	10	20×20	4	-NA-
mdb113	NORM	241	15	10	20×20	3	-NA-
mdb033	NORM	213	15	10	20×20	2	-NA-
mdb201	NORM	241	15	10	20×20	3	-NA-
mdb117	ARCH	237	15	10	20×20	2	Yes
mdb121	ARCH	231	15	10	20×20	3	Yes
mdb163	ARCH	234	15	10	20×20	4	Yes
mdb125	ARCH	230	15	10	20×20	3	No

As seen from Table 1 the proposed methodology is able to report architectural distortion in 4/5 cases which means that the proposed methodology scores high on the parameter of having low false negative rate. However the number of false positive per image is 2.8, which is bit high.

3.1 Summary

The results are shown for 10 mammograms taken from mini-MIAS database. The parameters t (number of iso-levels considered) and R (neighborhood) are obtained experimentally. The average number of false-positive per image points to the need for improvement. In the next chapter conclusions and future scope of the project is discussed.

Chapter IV
Conclusions and Future Scope

Conclusions and Future Scope

This project presents a new approach to find architectural distortions in mammograms based on the contour map and the concentration index. The results obtained are compared with the information available along with the mammograms, and it is felt that the proposed methodology holds promise. At this stage it is far from optimal, and needs to be rigorously tested with wide variety of mammograms from different databases. Moreover the current work focuses only on the architectural distortion present within the breast and does not take into consideration cancers around skinline [24]. The approach need to be extended to include skinline cancers also.

The algorithm at this stage of development has a significant number of false positive per image; other measures like isotropy index, size of suspicious site, contrasts, pixel values etc need to be explored to reduce the rate of false positive by utilizing more and more information present in the mammogram. A useful extension could be the coupling of the methodology with a classification scheme like neural network.

Appendix A

Following are the 16 arrangements for which the center pixel in 3×3 neighborhood is defined to be connecting pixel.

0 1 0	0 1 0	0 1 0	1 0 0
0 1 0	0 1 0	0 1 0	0 1 0
0 1 0	1 0 0	0 0 1	0 1 0
(1)	(2)	(3)	(4)

0 0 1	0 0 0	0 0 1	0 0 0
0 1 0	1 1 1	1 1 0	1 1 0
0 1 0	0 0 0	0 0 0	0 0 1
(5)	(6)	(7)	(8)

1 0 0	0 0 0	1 0 0	0 0 1
0 1 1	0 1 1	0 1 0	0 1 0
0 0 0	1 0 0	0 0 1	1 0 0
(9)	(10)	(11)	(12)

0 0 1	1 0 0	0 0 0	1 0 1
0 1 0	0 1 0	0 1 0	0 1 0
0 0 1	1 0 0	1 0 1	0 0 0
(13)	(14)	(15)	(16)

References

- [1] <http://www.imaginis.com/breasthealth/statistics.asp>,
http://www.imaginis.com/breasthealth/digital_mammo_print.asp the
breast cancer resource.
- [2] “Canadian cancer statistics 2004,” National Cancer Institute of
Canada, Toronto, Canada, 2004. [Online]. Available:
[http://www.cancer.ca/vgn/images/portal/cit_86751114/14/33/
195986411niw_states2004_en.pdf](http://www.cancer.ca/vgn/images/portal/cit_86751114/14/33/195986411niw_states2004_en.pdf).
- [3] Levi, F., F. Lucchini, E. Negri and C. La Vecchia. Trends in mortality
from major cancers in the European Union, including acceding countries,
in 2004. *Cancer* 101(12):2843.2850.
- [4] M.A. Schneider, “Better detection: Improving our chances,” in
*Digital Mammography: Proc. of the 5th Int. Workshop on Digital
Mammography*, Toronto, Canada: Medical Physics Publishing, 2000, pp.
3–6.
- [5] S.H. Heywang-Köbrunner, I. Schreer, and D.D. Dershaw, *Diagnostic
Breast Imaging: Mammography, Sonography, Magnetic Resonance
Imaging, and Interventional Procedures*. New York: Thieme Medical
Publishers, 1997.
- [6] *Illustrated breast imaging reporting and data system (BI-RADS)*, 3rd
ed., American College of Radiology, Reston, VA, 1998.

[7] J.A.A.M. van Dijck, A.L.M. Verbeek, J.H.C.L. Hendriks, and R. Holland, “The current detectability of breast cancer in a mammographic screening program,” *Cancer*, vol. 72, no. 6, pp. 1933–1938, 1993

[8] H.C. Burrell, D.M. Sibbering, A.R.M. Wilson, S.E. Pinder, A.J. Evans, L.J. Yeoman, C.W. Elston, I.O. Ellis, R.W. Blamey, and J.F.R. Robertson, “Screening interval breast cancers: Mammography features and prognostic factors,” *Radiology*, vol. 199, no. 7, pp. 811–817, 1996.

[9] E.A. Sickles, “Mammographic features of 300 consecutive nonpalpable breast cancers,” *American Journal of Roentgenology*, vol. 146, no. 12, pp. 661–663, 1986.

[10] M.J.M. Broeders, N.C. Onland-Moret, H.J.T.M. Rijken, J.H.C.L. Hendriks, A.L.M. Verbeek, and R. Holland, “Use of previous screening mammograms to identify features indicating cases that would have a possible gain in prognosis following earlier detection,” *European Journal of Cancer*, vol. 39, pp. 1770–1775, 1993.

[11] K. Kerlikowske, P.A. Carney, B. Geller, M. T. Mandelson, S. H. Taplin, K. Malvin, V. Ernster, N. Urban, G. Cutter, R. Rosenberg, and R. Ballard-Barbash, “Performance of screening mammography, among woman with and without a first-degree relative with breast cancer”, *Annals of Internal Medicine*, vol. 133, pp. 855-63, 2000.

[12] T. M. Kolb, J. Lichy, and J. H. Newhouse, “Comparison of performance of screening mammography, physical examination, and breast US and evaluation of factors that influence them: an analysis of 27,825 patient evaluation,” *Radiology*, vol. 255, pp. 165-75, 2002”.

- [13] R. E. Bird, T. W. Wallace, and B. C. Yankaskas, “ Analysis of cancers missed at screening mammography,” *Radiology.*, vol. 184, pp. 613-7, 1992.
- [14] M. L. Giger, “ Computer-Aided Diagnosis in radiology”, *Academic Radiology*, vol. 9, pp. 1-3, 2002.
- [15] D. B. Kopans, “The positive predictive value of mammography”, *AJR, American Journal of Roentgenology*, vol. 158, pp. 521-6, 1992.
- [16] <http://peipa.essex.ac.uk/info/mias.html> The mini-MIAS database of mammograms.
- [17] Fabio J. Ayres and Rangaraj M. Rangayyan, “Characterization of Architectural Distortion in Mammograms”, *IEEE Engenerring in Medicine and Biology Magazine*, January/February 2005.
- [18]N. Eltonsy, G. Tourassi and A. Elmaghraby, “Investigating performance of morphology based CAD scheme in detecting architectural in screening mammograms”.
- [19] Q. Guo, J. Shao and V. Ruiz, “Investigation of support vector machine for the detection of architectural distortion in mammographic images”, 2005 IOP Publishing Ltd.

[20] Gorgia D Tourassi, David m DeLong and Carey E Floyd Jr, “A study on the computerized fractal analysis of architectural distortion in screening mammograms”, 2006 IOP Publishing Ltd.

[21] Gary J. Whitman, Mehul P. Sampat, Mia K. Markey and Alan C. Bovik, “Evidence based detection of spiculated masses and architectural distortions”.

[22]Essam A. Rashed and Mohmad G. Awad, “Neural Network approach for mammography diagnosis using wavelet features”.

[23] Osmar R. Zaiane, Maria-Luzia Antonie and Alexendru Coman, “Mammography classification by an Association Rule-based Classifier”.

[24]T. Matsubara, T. Ichikawa, T. Hara, H. Fujita, S. Kasai, T. Endo and T. Iwase, “Automated detection methods for architectural distortions around skinline and within mammary gland on mammograms”.

[25] T. Matsubara, T. Ichikawa, T. Hara, H. Fujita, S. Kasai, T. Endo and T. Iwase, “Novel Method for detecting mammographic architectural distortion based on concentration of mammary gland”.

[26] T. Matsubara, D. Fukuoka, N. Yagi, T. Hara, H. Fujita, Y. Inenaga, S. Kasai, A. Kano, T. Endo and T. Iwase, “Detection method for architectural distortion based on analysis of structure of mammary gland on mammograms”.

[27] Digital Image Processing, Rafael C. Gonzales and Richard E. Woods, Addison Wesley, Ch. 8 pp. 535-38.

[28] A New Filter for Feature Extraction of Line Pattern Texture with Application to Cancer Detection. Jun-ichi Hasegawa & Jun-ichiro Toriwaki.

[29]T. Negoro, J. Toriwaki, and T.Fukumura, “A method for classification of point elements in line drawing patterns”, Trans.IECE, Japan, 55-D, 11, pp.762-763 (1972).